Revealing Equilibrium and Rate Constants of Weak and Fast Noncovalent Interactions

ARTICLE *in* ANALYTICAL CHEMISTRY · FEBRUARY 2011

Impact Factor: 5.64 · DOI: 10.1021/ac200010u · Source: PubMed

4 AUTHORS, INCLUDING:

Gleb G Mironov
University of Ottawa
13 PUBLICATIONS **66** CITATIONS
SEE PROFILE

Victor Okhonin
Custoiometrics Inc.
66 PUBLICATIONS **824** CITATIONS
SEE PROFILE

Maxim V Berezovski
University of Ottawa
73 PUBLICATIONS **2,007** CITATIONS
SEE PROFILE

analytical chemistry

ARTICLE

pubs.acs.org/ac

Revealing Equilibrium and Rate Constants of Weak and Fast Noncovalent Interactions

Gleb G. Mironov,[†] Victor Okhonin,[†] Serge I. Gorelsky,[†,‡] and Maxim V. Berezovski*[,†]

[†]Department of Chemistry, University of Ottawa, 10 Marie Curie, Ottawa, Canada K1N 6N5

[‡]Centre for Catalysis Research and Innovation, University of Ottawa, 30 Marie Curie, Ottawa, Canada K1N 6N5

Supporting Information

ABSTRACT: Rate and equilibrium constants of weak noncovalent molecular interactions are extremely difficult to measure. Here, we introduced a homogeneous approach called equilibrium capillary electrophoresis of equilibrium mixtures (ECEEM) to determine k_{on}, k_{off}, and K_d of weak (K_d > 1 μM) and fast kinetics (relaxation time, τ < 0.1 s) in quasi-equilibrium for multiple unlabeled ligands simultaneously in one microreactor. Conceptually, an equilibrium mixture (EM) of a ligand (L), target (T), and a complex (C) is prepared. The mixture is introduced into the beginning of a capillary reactor with aspect ratio >1000 filled with T. Afterward, differential mobility of L, T, and C along the reactor is induced by an electric field. The combination of differential mobility of reactants and their interactions leads to a change of the EM peak shape. This change is a function of rate constants, so the rate and equilibrium constants can be directly determined from the analysis of the EM peak shape (width and symmetry) and propagation pattern along the reactor. We proved experimentally the use of ECEEM for multiplex determination of kinetic parameters describing weak (3 mM > K_d > 80 μM) and fast (0.25 s ≥ τ ≥ 0.9 ms) noncovalent interactions between four small molecule drugs (ibuprofen, *S*-flurbiprofen, salicylic acid and phenylbutazone) and α- and β-cyclodextrins. The affinity of the drugs was significantly higher for β-cyclodextrin than α-cyclodextrin and mostly determined by the rate constant of complex formation.

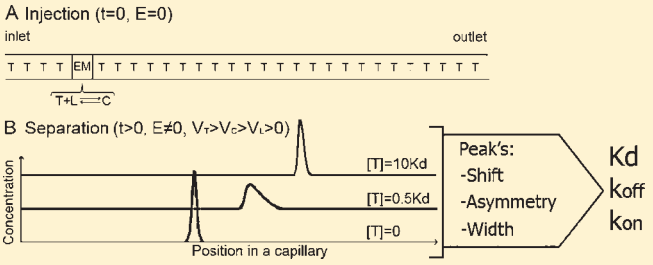

Measuring rate and equilibrium constants of molecular noncovalent interactions is important for the understanding of drug actions and cellular processes.[1−3] The dissociation rate of drug−protein complexes may be the limiting step for drug elimination and tissue distribution. Only the unbound drug is available for diffusion from plasma into organs and for reaction with cellular targets.[2,4] For example, fast binding rates allow ligands to activate immune T cells more effectively than slow ligands and demonstrate a strong stimulatory effect.[1]

The determination of rate constants is very difficult for a fast binary reaction where a ligand (L) binds reversibly to a target (T) forming a complex (C):

$$\mathrm{L} + \mathrm{T} \underset{k_{off}}{\overset{k_{on}}{\rightleftharpoons}} \mathrm{C} \qquad K_d = k_{off}/k_{on} \tag{1}$$

where k_{on} and k_{off} are rate constants of forward and reverse processes, respectively, and K_d is the equilibrium dissociation constant. The relaxation time τ to equilibrium for weak (K_d > 1 μM) reactions is usually less than a second and depends on rate constants and ligand (L) and target (T) concentrations:

$$\tau = 1/(k_{on}(L+T) + k_{off}) \tag{2}$$

The major existing methods studying noncovalent molecular interaction kinetics are stopped-flow (SF) and surface plasmon resonance (SPR) with the minimum τ of 0.001 and 0.1 s, respectively.[5,6] These methods fail to measure faster rates because of mixing dead-time and redissociation of reagents for SF as well as mass transport to and heterogeneity of the surface of a SPR chip.[7,8] The kinetics of such interactions in SF and SPR are studied by monitoring the changes in the reactant/product concentration after the reaction is significantly perturbed from an equilibrium.[9]

In our work, we introduce the first homogeneous approach to determine k_{on}, k_{off}, and K_d of weak and fast kinetics in quasi-equilibrium for multiple unlabeled ligands simultaneously in one microreactor. At the conceptual level, an equilibrium mixture (EM) of L, T, and C is prepared. The mixture is introduced into the beginning of a long and narrow capillary reactor filled with T. Afterward, differential mobility of L, T, and C along the reactor is induced by an external action such as an electric field. The combination of differential mobility of reactants and their interaction leads to a change of the EM peak position and shape. The change is a function of rate constants, so that the rate and equilibrium constants are directly determined from the analysis of the propagation pattern and the shape of the EM peak along the reactor.

Received: January 3, 2011
Accepted: January 29, 2011
Published: February 24, 2011

In this work, we apply a method called equilibrium capillary electrophoresis of equilibrium mixtures (ECEEM).[10] It is a member of kinetic capillary electrophoresis (KCE), a platform for kinetic homogeneous affinity methods in which molecules interact with each other during electrophoretic separation.[11] Previously, ECEEM was used only for determination of K_d and selection of "smart" affinity probes (aptamers and DNA-tagged small molecules) with desirable K_d values.[10,12,13] The quasi-equilibrium nature of ECEEM allows us to find an approximated analytical solution of mass transfer equations. We use this solution to simulate and study spatial and temporal propagation patterns of L and C for different T concentrations. We then develop a parameter-based method for finding the rate constants of complex formation and dissociation from experimental electropherograms. Finally, we demonstrate the use of ECEEM for determining kinetic parameters of noncovalent interactions between four small molecule drugs (ibuprofen, *S*-flurbiprofen, salicylic acid, and phenylbutazone) as ligands and α- and β-cyclodextrins as targets. A long silica capillary is used as a microreactor; a diode-array detector is used for detection of the unlabeled small molecules, and an electric field is used to induce differential mobility. The measurements are performed by a commercial capillary electrophoresis instrument without modifications, suggesting that ECEEM can be immediately and widely practiced.

RESULTS

Principle of ECEEM. Practically, in ECEEM, an equilibrium mixture of a target with one or multiple ligands is prepared and equilibrated. A plug of EM is injected into a capillary prefilled with a run buffer containing T with a total concentration identical to EM (Figure 1A). Components of EM are separated by capillary electrophoresis while quasi-equilibrium is maintained between T, L, and C inside the capillary. There are three unique features of ECEEM: (i) the migration time of the EM peak depends on concentration of T in the run buffer, so ligands with different K_d values migrate with different velocities; (ii) L and C migrate as a single EM peak due to fast exchange between them; and (iii) EM peak broadening is dependent on concentration of T, relaxation time τ, and characteristic separation time. The characteristic separation time, t_{sep}, is the time required for L and C to separate from each other and can be defined as:

$$t_{sep} = w/(2|V_C - V_L|) \quad (3)$$

where w is the width of the initial EM peak and V_C and V_L are the velocities of C and L, respectively. If $\tau > t_{sep}$, the zones of L and C are separated before the re-equilibration in reaction 1 proceeds to a significant extent. Thus, L and C are moving as separate peaks. If $\tau \sim t_{sep}$, re-equilibration in reaction 1 and separation proceed with comparable rates. Therefore, L and C are moving as two peaks with some overlap between them. Finally, if $\tau < t_{sep}$, the re-equilibration in reaction 1 occurs much faster than peak separation, and as a result, L and C will be moving as a single peak. The last case of fast molecular interactions is conceptually illustrated in Figure 1. The figure shows spatial propagation patterns of L and C for the three different concentrations of T (T = 0, 0.5K_d, and 10K_d). When T = 0 (Figure 1B top panel), C completely dissociates in the first seconds, so EM migrates as a Gaussian symmetrical peak with the velocity of free L. When T = 0.5K_d (Figure 1B middle panel), EM contains L and C in a 1:2 ratio and moves as a single peak with an intermediate velocity V_{EM} ($V_C > V_{EM} > V_L$). At the same time, the peak becomes asymmetrical and wider than free L. The asymmetry of the peak is caused by the nonlinear effect of complex formation due to the gradient of T inside the EM peak. In Figure 1B bottom panel, the concentration of T is so high (T = 10K_d) that the majority of L presents in C and migrates with V_C. The shape of the peak becomes symmetrical again, and the width is similar with free L.

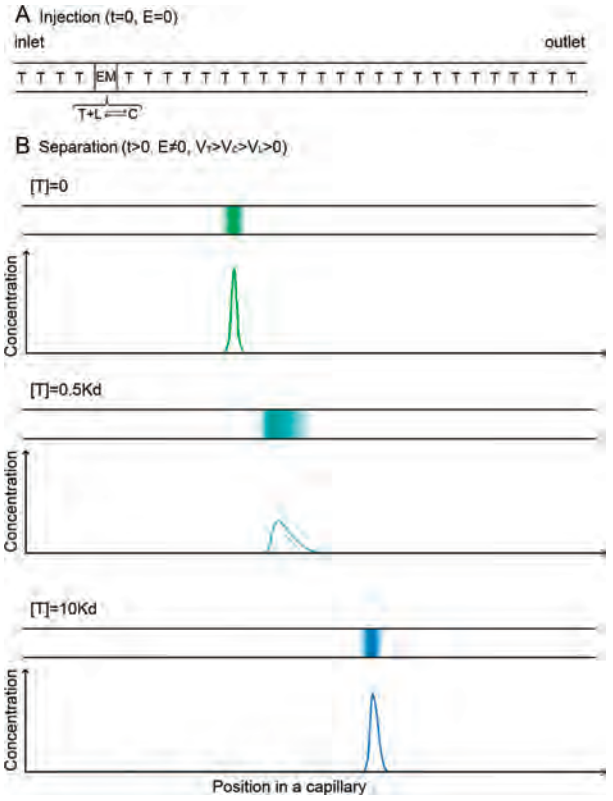

Figure 1. (A) Schematic representation of ECEEM setup in its initial condition. (B) Illustration of spatial propagation patterns of a ligand (L, green) and a complex (C, blue) in a single-dimensional reactor at different target concentrations (T, white).

Analytical Solutions of Mass Transfer Equations in ECEEM. The ECEEM separation of three reactants in capillary electrophoresis is described by the system of mass transfer equations:

$$\frac{\partial L}{\partial t} + V_L\frac{\partial L}{\partial x} - D_L\frac{\partial^2 L}{\partial x^2} = \frac{\partial T}{\partial t} + V_T\frac{\partial T}{\partial x} - D_T\frac{\partial^2 T}{\partial x^2} =$$

$$= k_{off}C - k_{on}LT = -\frac{\partial C}{\partial t} - V_C\frac{\partial C}{\partial x} + D_C\frac{\partial^2 C}{\partial x^2} \quad (4)$$

where L, T, and C are the concentrations of a ligand, target, and complex, respectively, V_L, V_T, and V_C are the migration velocities, D_L, D_T, and D_C are the coefficients of diffusion, t is the time, x is the spatial coordinate, k_{off} is the decay constant, and k_{on} is the rate constant of complex formation.

The general analytical solution of these nonlinear differential equations in partial derivatives is not known. In some cases when (i) formation or decay rate constants are negligible or zero[14,15] or (ii) $V_C = V_L$ or $V_C = V_T$ (this case is described in Supporting Information), the eq 4 becomes linear directly or after the

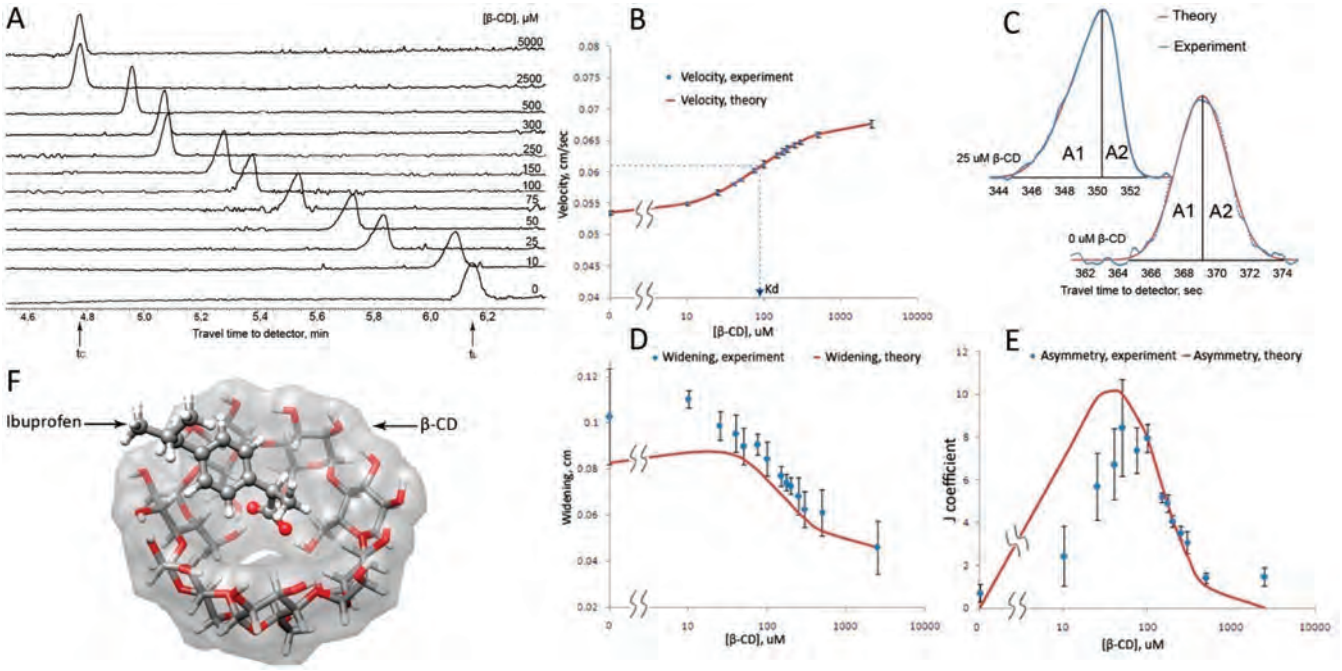

Figure 2. Determination of equilibrium and rate constants of β-CD/ibuprofen. (A) Representative ECEEM electropherograms of ibuprofen (30 μM) for varying concentration of β-CD. (B) The plot of EM velocity as a function of β-CD concentration for K_d determination. (C) Representative shapes of free ligand and EM peaks (theoretical and experimental). (D) Dependence of EM peak widening ($\Delta - \Delta_0$) on the concentration of β-CD. (E) Dependence of EM peak asymmetry, J, on the concentration of β-CD. (F) The visualization of a DFT calculated β-CD/ibuprofen complex.

Cole-Hopf substitution.[16,17] For our case of fast molecular exchange ($\tau < t_{sep}$) and $L < T + K_d$, the following approximated equation can be used

$$\partial_t L + \left(V_{EM} - \frac{2k_{on}D_{CID}}{V_T - V_{EM}}L\right)\partial_x L \approx (D_{CID} + D_{EM})\partial_x{}^2 L \quad (5)$$

where V_{EM} is the velocity of EM peak, D_{EM} is a physical diffusion coefficient for EM peak, and D_{CID} is a chemical induced coefficient of diffusion. They can be described as:

$$V_{EM} \equiv \frac{K_d V_L + TV_C}{K_d + T}, \quad D_{EM} \equiv \frac{K_d D_L + TD_C}{K_d + T},$$
$$D_{CID} \equiv \frac{TK_d{}^2(V_C - V_L)^2}{k_{off}(K_d + T)^3} \quad (6)$$

Equation 5 is well-known in mathematics as Burgers' equation. The special exact solution of Burgers' equation is following

$$L + C = \frac{\Delta \equiv \sqrt{\Delta_0^2 + 4t(D_{EM} + D_{CID})},}{\sqrt{\pi}/\left(\exp\left(\frac{k_{off}D_{CID}L_0 \times l}{|V_T - V_{EM}|(K_d + T)(D_{CID} + D_{EM})}\right) - 1\right) + \int_{-\infty \cdot sign(V_T - V_{EM})}^{x - V_{EM}t/\Delta} \exp(-y^2)dy} \quad (7)$$

where Δ and Δ_0 are a Gaussian half-width (STD $(2)^{1/2}$) of the EM peak at $t > 0$ and $t = 0$, respectively, after the Cole-Hopf transformation which "linearizes" Burgers' equation. In other words, an asymmetrical peak becomes symmetrical after the Cole-Hopf transformation. L_0 is the total concentration of the ligand in EM, and l is a plug length of the EM injection. Solution 7 corresponds to initial conditions when the initial EM peak is sharp or the peak becomes a Gaussian after the Cole-Hopf transformation. In the case when L_0 is very low and $L_0 \times l \ll |V_T - V_{EM}|(K_d + T)/K_{off}$, solution 7 becomes close to a Gaussian distribution and does not require the Cole-Hopf transformation.

The asymmetry of the EM peak J is defined by a factor r, a ratio of the bigger area (A_1) to the smaller area (A_2) of the EM peak divided at its maximum (Figure 2C). There is an approximated connection between r and the rate and equilibrium constants:

$$J \equiv \frac{k_{off}D_{CID}L_0 \times l}{|V_T - V_{EM}|(K_d + T)(D_{CID} + D_{EM})} \approx$$
$$\approx 5.499 \cdot (r - 1)^{0.87925} \cdot \exp((r - 1) \cdot 0.0289) \quad (8)$$

dx.doi.org/10.1021/ac200010u |Anal. Chem. 2011, 83, 2364–2370

K_d can be found from the expression:

$$K_d \approx \sum_i \frac{(V^i_{EM} - V_L)^3 (V_C - V^i_{EM})}{T_i} \Big/ \sum_i \frac{(V_L - V^i_{EM})^4}{T_i^2} \quad (9)$$

When J, V_C, V_L, V_T, D_C, D_L, and K_d are known, k_{off} can be determined from eq 8. For the low asymmetry case ($r \sim 1$), k_{off} can be found from the EM peak widening using eq 7. More detailed math derivations are described in Supporting Information.

Experimental Model. An experimental model involving the formation of inclusion complexes between α- and β-cyclodextrins (CDs) and small organic molecules (SMs) was chosen as a representative and important example of weak and fast affinity noncovalent interactions. Four well-known anti-inflammatory drugs: ibuprofen, *S*-flurbiprofen, salicylic acid, and phenylbutazone form a host−guest complex with cyclodextrins. Visual structures of the complexes are presented in Figures 2F (for β-CD/ibuprofen) and S2 (Supporting Information, for α- and β-CD/SMs). The formation of inclusion complexes modifies the physical and chemical properties of guest small molecules and significantly increases their water solubility. This is the reason why CDs attract interest in pharmaceutical applications.[18] CDs enhance the bioavailability of poorly soluble drugs by delivering a hydrophobic drug to a lipid cell membrane, where the drug can penetrate inside a cell.[19] Therefore, measuring kinetics of complex dissociation and association between CDs and drugs is extremely important for understanding drug actions. Fast kinetics with high affinity increases the drug activity by enhancing its solubility and the fraction of an administered dose of the drug that reaches the systemic circulation. Reciprocally, slow kinetics and low affinity decrease its activity. In this proof-of-principle work, we conducted the study in a narrow (inner diameter of 75 μm) and long 89 cm (29 cm for ibuprofen) capillary reactor. We chose an electric field to induce differential mobility of L and C. Radial gradients of concentrations and radial mass transfer are negligible in such a 1-dimensional capillary reactor. To exclude boundary effects in a finite-length capillary reactor, the ends of the capillary were placed into reservoirs with the running buffer containing T. Advantageously, commercial capillary electrophoresis instruments with UV or photodiode array (PDA) detection can be used for such experiments. They are typically equipped with single-point detectors (located close to the end of the capillary) recording temporal label-propagation patterns. In this work, we used one such instrument without any modifications.

To stay consistent with the terminology used in the theoretical consideration, α- and β-cyclodextrins are called T, while the small molecules are called L. Their complexes are called C.

We have a few important notes on the choice of experimental conditions. The experimental conditions for the CD/SM system were chosen to minimize the potential effect of the formation of a complex of a small molecule with two molecules of CD. We used a range of concentrations of β-CD (10 μM to 5 mM) well below concentrations of β-CD (>10 mM) at which the formation of 2:1 β-CD/SM complex was observed.[20]

Experimental Parameter-Based Method for Determination of K_d, k_{on}, and k_{off} for One Interaction Pair. Time propagation profiles of C and L propagation for the experimental model β-CD/ibuprofen were studied for varying concentrations of β-CD (Figure 2A). CD molecules are bulky and neutral, so electroosmotic flow moves them faster than SM molecules. The mobility of the complex is between CD and SM and can be found by the mobility of the EM peak at high concentration of CD using the dependence on EM velocity and concentration of β-CD (Figure 2B). A notable shift of the EM zone was observed with the increase of T.

To determine k_{on} and k_{off} for our experimental model, we used the parameter-based method, the theory of which was described earlier. The process of finding binding constants can be divided into four steps: (i) measuring velocities of L, C, and T, (ii) calculating K_d, (iii) finding J (EM peak asymmetry), and (iv) finally calculating k_{off}.

Rate and equilibrium constants were determined for the ibuprofen/β-CD system: k_{off} = 12.7 ± 1.7 s^{-1}, K_d = 86.1 ± 1.4 μM, and k_{on} = (14.8 ± 2.3) × 10^4 $M^{-1}s^{-1}$. To the best of our knowledge, this is the first report on the kinetic parameters for the fast ($\tau \sim 1.9$ ms) small organic molecule/cyclodextrin interaction. This molecular pair also has prominent pharmacological importance.[18] The constants were calculated on the basis of 15 experiments repeated three times each with a fixed concentration of ibuprofen (30 μM) and varying concentrations of β-CD from 10 μM to 5 mM. Experiments carried out with T in the range of (0.1−3) × K_d provide the most confident results of rate and equilibrium constants. In this range, the EM contains both L and C in comparable amounts. The behavior of the confidence for β-CD/ibuprofen complex formation is presented in Figure S1, Supporting Information.

It should be mentioned that molecular diffusion can contribute to zone widening in a similar way as molecular interaction. Moreover, in our case, the zone became broader with decreasing migration time; the phenomenon opposite to that could be caused by diffusion. Nevertheless, we found diffusion coefficients for L and C by a CE method described elsewhere.[21] Briefly, we measured the change of either L (at T = 0 in the run buffer) or C (at high T) peak profiles in the same CE experiment: before dispersion and after dispersion of an injected plug. This was achieved by first moving an analyte in one direction to pass the detector and record the initial concentration profile. The analyte was then stopped to allow for its diffusion. Finally, the analyte was moved back to pass the detector for the second time and record the final concentration profile. The diffusion coefficients for free ibuprofen and its complex were 4.6 × 10^{-6} and 1.7 × 10^{-6} cm^2sec^{-1}, respectively.

A computer simulated model of the complex between ibuprofen and β-CD is shown in Figure 2F. According to this DFT-calculated model, CD holds ibuprofen inside the cavity by two hydrogen bonds between a terminal carboxyl group of ibuprofen and two hydroxyl groups on the bottom of the cyclic oligosaccharide.

Simultaneous Determination of K_d, k_{on}, and k_{off} for Multiple Interaction Pairs. The experimental setup and calculation procedures of finding rate and equilibrium constants for multiple CD/SM pairs were the same as for the previously described β-CD/ibuprofen pair. The only differences were the longer length of the capillary (89 cm) and the injected EM contained all four SMs. As long as electropherograms provide necessary information (a velocity, area, and shape) about all peaks, it is possible to measure binding constants, so the maximum number of compounds studied with this method is limited only by resolution of the CE separation, which was ∼60.

We studied time profiles of peak propagation for two experimental models: a mixture of phenylbutazone, ibuprofen, *S*-flurbiprofen, and salicylic acid with either α-CD or β-CD. The experimental electropherograms for varying concentrations of

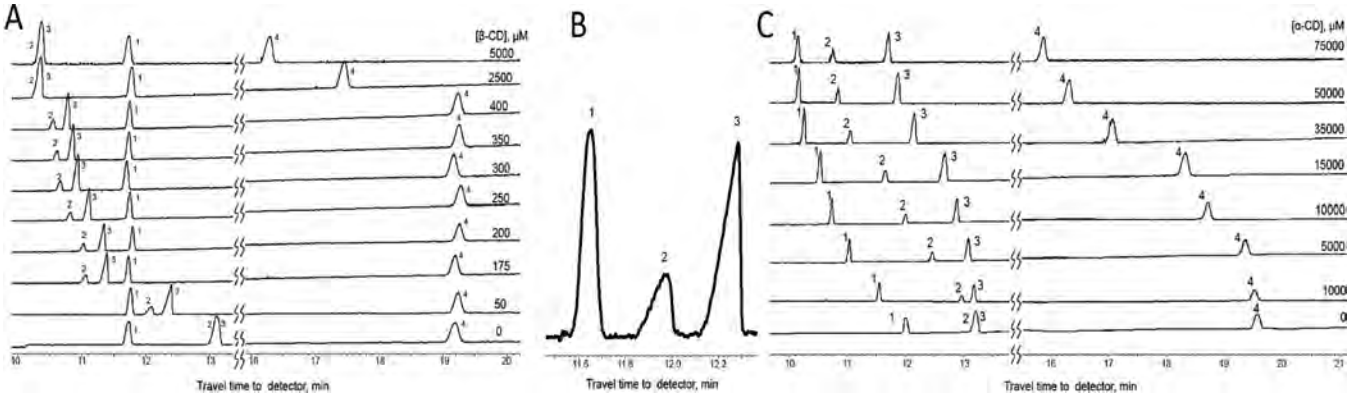

Figure 3. ECEEM of mixture of 30 μM phenylbutazone (1), 30 μM ibuprofen (2), 30 μM *S*-flurbiprofen (3), and 50 μM salicylic acid (4) in 50 mM Tris−acetate buffer with various concentrations of β-CD (A) and α-CD (C). Observed peak shapes for 30 μM phenylbutazone (1), 30 μM ibuprofen (2), and 30 μM *S*-flurbiprofen (3) in 50 mM Tris−acetate buffer with 50 μM β-CD (B).

Table 1. Rate and Equilibrium Constants between Small Molecules and Cyclodextrins Measured in Multiplex Experiments

α-CD (β-CD)	*S*-flurbiprofen	ibuprofen	salicylic acid	phenylbutazone
K_d, μM	19 000 ± 4000 (155 ± 2)	12 000 ± 1500 (80 ± 17)	26 000 ± 3000 (3200 ± 700)	4500 ± 800
k_{on}, $\times 10^3$ $M^{-1}s^{-1}$	0.3 ± 0.1 (210 ± 30)	0.8 ± 0.4 (102 ± 9)	0.3 ± 0.1 (1.3 ± 0.4)	1.2 ± 0.3
k_{off}, s^{-1}	6.0 ± 0.7 (33 ± 5)	9.5 ± 2.8 (8.4 ± 1.2)	6.5 ± 0.9 (4.3 ± 1.7)	5.4 ± 0.7
complex's lifetime, ms	166 ± 16 (31 ± 5)	104 ± 24 (119 ± 15)	155 ± 18 (230 ± 7)	185 ± 22

α-CD and β-CD are shown in Figure 3C, A, respectively. The increase of CD concentration decreases the migration times of SMs and the change of their peak shapes. For example, peak 2 (ibuprofen) and peak 3 (*S*-flurbiprofen) in Figure 3B are asymmetrical and wider than the symmetrical and narrow peak 1 (phenylbutazone) in the presence of 50 μM β-CD, because phenylbutazone does not form a complex.

We calculated all rate and equilibrium constants and presented them in Table 1 except for the β-CD/phenylbutazone pair. Phenylbutazone did not show any affinity to β-CD. Binding affinities of drugs to β-CD are higher than to α-CD by a factor of 145 for ibuprofen, 121 for *S*-flurbiprofen, and 8 for salicylic acid. Structural diversity between α-CD and β-CD causes the variation in rate constants of complex formation. The inner cavity of α-CD (3.9 Å at the bottom and 5.3 Å at the top) is smaller than that of β-CD (5.3 Å × 7.0 Å), so it takes longer for drugs to fit in and to form an inclusion complex with α-CD than with β-CD. The dissociation of complexes happens very quickly, and the lifetime of the complexes varies from 31 to 233 ms. We were able to measure the rate and equilibrium constants for very fast interactions with the relaxation time varying from 230 to 0.9 ms and K_d varying from 80 μM to 3 mM. Additional parameters of β-CD/SM interactions like relaxation time, life times of complexes, free SM and free β-CD were calculated and presented in Tables 1S, 2S, and 3S in the Supporting Information.

Cyclodextrins have a shape of a torus with a less hydrophilic cavity than the outside environment. To enter into the cavity ibuprofen, *S*-flurbiprofen and salicylic acid have to overcome steric hindrances and exclude water molecules from the inner space, but the formation of new hydrogen bonds between SM and the bottom of the cavity stabilizes these complexes. In our experiments, we observed a high affinity of ibuprofen and *S*-flurbiprofen binding to β-CD. *S*-flurbiprofen with two aromatic rings is bigger than ibuprofen which has only one ring. Interesting to note is that k_{on} for *S*-flurbiprofen is twice as high as that for ibuprofen, but the complex's lifetime is four times shorter. The big size of *S*-flurbiprofen probably makes it difficult to stay inside CD, so the complex dissociates very fast.

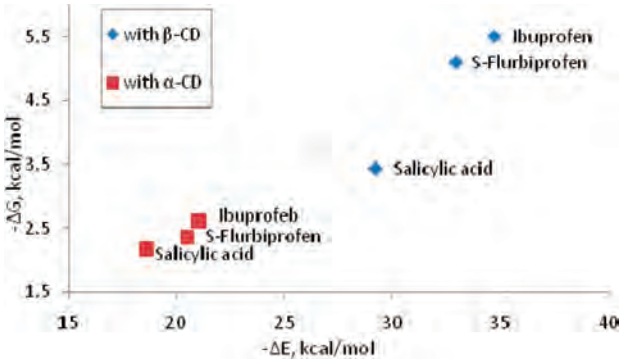

Figure 4. Correlation between experimental binding free energies, ΔG, obtained from K_ds and DFT-calculated electronic binding energies, ΔE, for α-CD/SM (red squares) and β-CD/SM (blue diamonds) complexes.

In addition, we performed DFT calculations for complexes between three drugs (ibuprofen, *S*-flurbiprofen, and salicylic acid) and cyclodextrins to find their structures (Figure S2, Supporting Information.). The calculated electronic binding energies (ΔE without entropy and thermal correlation) depend linearly with the Gibbs free energies (ΔG) obtained from experimentally determined equilibrium dissociation constants (Figure 4).

DISCUSSION

Kinetic capillary electrophoresis (KCE),[11] which started with the pioneering work of Whitesides on affinity capillary electrophoresis (ACE),[22−24] establishes a new homogeneous platform for studying kinetics and thermodynamics of molecular interactions. In KCE, differential mobility of T and L is used to

create conditions for measuring rate and equilibrium constants of their interactions. Most of the seven KCE methods (NECEEM, SweepCE, plug−plug KCE, etc.) are perturbations and not suitable for measuring reactions with fast re-equilibration ($\tau < t_{sep}$). This makes the perturbation methods inapplicable to fast reactions. For example, in NECEEM, if the dissociation of a complex happens quickly, it is almost impossible to measure $k_{off} > 0.1\ s^{-1}$.

In contrast, ECEEM considers both the forward and reverse process in reaction 1. ECEEM is a quasi-equilibrium method, in which a target fills the reactor and the propagation of one or multiple ligands through the target is followed while maintaining fast equilibrium. The method was originally used to find K_d only. However, Whitesides and coauthors suggested it for finding rate and equilibrium constants through a relatively complicated numerical approach of fitting reactant-propagation profiles.[23,24] The complexity of the analysis and the method's applicability to intermediate rates of equilibration ($\tau \sim 10$ s) likely explain why the method has never been utilized thereafter for 18 years.

In this study, we applied a simple experimental method, ECEEM, and revealed that peaks shift; it's asymmetry and widening can be used for the precise determination of rate constants for weak molecular interactions. There is no labeling procedure necessary. The equilibrium mixture of the unlabeled ligand and the target is injected into a "long" capillary and separated in the buffer containing the same concentration of the target. "Long" means there are no boundary effects at the entrance and exit points of the reactor, and "narrow" means there are no radial concentration gradients and mass transfer. For practical consideration, capillaries typically used in capillary electrophoresis and capillary chromatography have a length of 20−80 cm and an inner diameter of 20−75 μm and can be used as "long and narrow" reactors in all foreseeable experimental models.

In addition, ECEEM has an unique "accumulation" property. It accumulates the effect of molecular interactions through the change of peak shapes during the electrophoretic separation. Experiments in extra long capillaries could potentially reveal rates of extremely fast interactions by measuring width and asymmetry of EM peaks, if $D_{CID} > D_{EM}$.

While in our experimental demonstration of ECEEM we used an electric field, other means of inducing differential mobility can be used like chromatography or centrifugation. It is difficult to hypothesize on advantages and limitations of different ways of separation a priori but some general considerations can be made. An external action used in ECEEM to induce the differential mobility can potentially affect the reaction kinetics. We performed our separation experiments at different electric fields and found small variations (<25%) of binding constants. Nevertheless, the possibility of such an influence cannot be completely excluded and could be experimentally studied by varying an electric field and extrapolating the results to zero voltage. A similar concern exists for chromatography. The interaction of the reaction components with the chromatographic stationary phase can also affect the reaction kinetics. While PDA detection was used in our study, ECEEM is compatible with other types of detectors: fluorescent, electrochemical, and mass spectrometric.

To conclude, we developed a homogeneous method to determine k_{on}, k_{off}, and K_d of fast and weak noncovalent interactions between multiple unlabeled ligands (small molecule drugs) and an oligosaccharide (α- or β-cyclodextrin) simultaneously in one capillary microreactor. The availability of commercial instrumentation for capillary electrophoresis and high-performance liquid chromatography with all of the previously listed detection approaches suggests that ECEEM can be practiced immediately. ECEEM can potentially facilitate kinetic studies of noncovalent interactions with complicated stoichiometry (different from 1:1) involving proteins and nucleic acids.

MATERIALS AND METHODS

Chemicals and Materials. Chemicals were purchased from the following companies: salicylic acid (Santa Cruz Biotechnology, USA, cat. # sc-203374), (*S*)-flurbiprofen (Cayman Chemical, USA, cat. # 10004207), ibuprofen (Sigma Aldrich, Canada, cat.# I4883), phenylbutazone (Santa Cruz Biotechnology, cat. # sc-204843), α-cyclodextrin (USB Corporation, USA, cat.# 13979), and β-cyclodextrin (Sigma Aldrich, Canada, cat.# c4767). For all experiments, 50 mM Tris−Acetate, pH 7.85, was used as an incubation/run buffer. The buffer was prepared by dilution from 200 mM Tris−Acetate stock buffer. The stock buffer was made by dissolving 12.11 g of Tris-base (Bio Basic Inc., Canada, cat.# 77-86-1) and 2.86 mL of acetic acid (Bio Basic Inc., Canada, cat.# C1000) in 500 mL of ddH_2O.

Equilibrium mixtures of drugs and cyclodextrins were prepared in the incubation buffer with the following concentrations of small molecules: 30 μM *S*-flurbiprofen, 30 μM ibuprofen, 30 μM phenylbutazone, 50 μM salicylic acid, and cyclodextrins: 25 μM−5 mM β-cyclodextrin and 250 μM−100 mM α-cyclodextrin. Stock solutions (10 mM) of small molecules (except phenylbutazone) were prepared by directly dissolving a weighed amount of the drugs in 10 mL of the incubation buffer. For phenylbutazone, a 10 mM stock solution was prepared in 95% ethanol and then diluted in the incubation buffer. All solutions were filtered through 0.22 μm pore size membrane filters (Millipore, Nepean, ON, Canada).The bare-silica capillary was purchased from Polymicro (Phoenix, AZ, USA).

Experimental Conditions of ECEEM. All ECEEM experiments were performed with the following instrumentation, settings, and operations unless otherwise stated. ECEEM was carried out with a PA800 Pharmaceutical Analysis CE system (Beckman Coulter, USA) equipped with PDA and UV detectors. We used the following conditions: the sample storage and capillary temperature maintained at 25 ± 0.5 °C, an electric field of 303 V/cm (172 V/cm for the individual β-CD/ibuprofen pair) with a positive electrode at the injection end, the run buffer with one of the cyclodextrins in the inlet reservoir, and the incubation/run buffer in the outlet reservoir. The concentration of the cyclodextrin in the equilibrium mixture and the run buffer was the same for individual ECEEM experiments. For all experiments, the capillary was 89 cm long (80 cm to the detection window; for individual ibuprofen 29 and 20 cm, respectively) with an inner diameter of 75 μm and an outer diameter of 360 μm. An approximately 15 mm long plug (29.82 nL) of the equilibrium mixture was injected into the capillary from the inlet end by a pressure pulse of 8 s × 0.5 psi. Before each experiment, the capillary was rinsed by 20 psi pressure with 0.1 M HCl for 3 min, 0.1 M NaOH for 3 min, ddH_2O for 3 min, 50 mM Tris-Acetate buffer for 5 min, and the incubation/run buffer with cyclodextrin for 1 min. The output data was absorbance intensity in the detection point, as a function of time passed since the application of the electric field.

■ ASSOCIATED CONTENT

Supporting Information. Detailed analytical mathematical solutions for fast kinetics, modeled structures of CD/SM complexes, and tables of complex formation parameters. This material is available free of charge via the Internet at http://pubs.acs.org.

■ AUTHOR INFORMATION

Corresponding Author
*E-mail: maxim.berezovski@uottawa.ca.

■ ACKNOWLEDGMENT

This work was supported by Natural Sciences and Engineering Research Council of Canada.

■ REFERENCES

(1) Govern, C. C.; Paczosa, M. K.; Chakraborty, A. K.; Huseby, E. S. *Proc. Natl. Acad. Sci. U.S.A.* **2010**, *107*, 8724–8729.
(2) Berezhkovskiy, L. M. *Expert Opin. Drug Metab. Toxicol.* **2008**, *4*, 1479–1498.
(3) Goyal, M.; Rizzo, M.; Schumacher, F.; Wong, C. F. *J. Med. Chem.* **2009**, *52*, 5582–5585.
(4) Berezhkovskiy, L. M. *J. Pharm. Sci.* **2006**, *95*, 834–848.
(5) Brissette, P.; Ballou, D. P.; Massey, V. *Anal. Biochem.* **1989**, *181*, 234–238.
(6) Wild, M. K.; Huang, M. C.; Schulze-Horsel, U.; van der Merwe, P. A.; Vestweber, D. *J. Biol. Chem.* **2001**, *276*, 31602–31612.
(7) Fabian, H.; Naumann, D. *Methods* **2004**, *34*, 28–40.
(8) Piliarik, M.; Vaisocherova, H.; Homola, J. *Methods Mol. Biol.* **2009**, *503*, 65–88.
(9) Bujalowski, W. *Chem. Rev.* **2006**, *106*, 556–606.
(10) Drabovich, A.; Berezovski, M.; Krylov, S. N. *J. Am. Chem. Soc.* **2005**, *127*, 11224–11225.
(11) Petrov, A.; Okhonin, V.; Berezovski, M.; Krylov, S. N. *J. Am. Chem. Soc.* **2005**, *127*, 17104–17110.
(12) Drabovich, A. P.; Berezovski, M.; Okhonin, V.; Krylov, S. N. *Anal. Chem.* **2006**, *78*, 3171–3178.
(13) Drabovich, A. P.; Berezovski, M. V.; Musheev, M. U.; Krylov, S. N. *Anal. Chem.* **2009**, *81*, 490–494.
(14) Berezovski, M.; Krylov, S. N. *J. Am. Chem. Soc.* **2002**, *124* 13674–13675.
(15) Okhonin, V.; Petrov, A. P.; Berezovski, M.; Krylov, S. N. *Anal. Chem.* **2006**, *78*, 4803–4810.
(16) Cole, J. D. *Quart. Appl. Math.* **1951**, *9*, 225–236.
(17) Hopf, E. *Comm. Pure Appl. Math.* **1950**, *3*, 201–230.
(18) Li, D. X.; Han, M. J.; Balakrishnan, P.; Yan, Y. D.; Oh, D. H.; Joe, J. H.; Seo, Y.; Kim, J. O.; Park, S. M.; Yong, C. S.; Choi, H. G. *Arch. Pharm. Res.* **2010**, *33*, 95–101.
(19) Loftsson, T.; Vogensen, S. B.; Brewster, M. E.; Konradsdottir, F. *J. Pharm. Sci.* **2007**, *96*, 2532–2546.
(20) Loftsson, T.; Magnusdottir, A.; Masson, M.; Sigurjonsdottir, J. F. *J. Pharm. Sci.* **2002**, *91*, 2307–2316.
(21) Musheev, M. U.; Javaherian, S.; Okhonin, V.; Krylov, S. N. *Anal. Chem.* **2008**, *80*, 6752–6757.
(22) Chu, Y. H.; Avila, L. Z.; Biebuyck, H. A.; Whitesides, G. M. *J. Med. Chem.* **1992**, *35*, 2915–2907.
(23) Avila, L. Z.; Chu, Y. H.; Blossey, E. C.; Whitesides, G. M. *J. Med. Chem.* **1993**, *36*, 126–133.
(24) Chu, Y.-H.; Avila, L. Z.; Gao, J.; Whitesides, G. M. *Acc. Chem. Res.* **1995**, *28*, 461–468.

SUPPORTING INFORMATION

Revealing Equilibrium and Rate Constants of Weak and Fast Non-Covalent Interactions

Gleb Mironov, Victor Okhonin, Serge I. Gorelsky and Maxim V. Berezovski*

Department of Chemistry, University of Ottawa, 10 Marie Curie, Ottawa, Canada K1N 6N5;

*To whom correspondence may be addressed. E-mail: maxim.berezovski@uottawa.ca

Table of Contents

Supporting Analytical Solution for Kinetics

1. General mass transfer equations

Precise equations describing a binary reverse reaction happening during capillary electrophoresis - based separation are the following:

$$\frac{\partial \boldsymbol{L}}{\partial \boldsymbol{t}}+\boldsymbol{V}_{\boldsymbol{L}}\frac{\partial \boldsymbol{L}}{\partial \boldsymbol{x}}-\boldsymbol{D}_{\boldsymbol{L}}\frac{\partial^2 \boldsymbol{L}}{\partial \boldsymbol{x}^2}=\frac{\partial \boldsymbol{T}_0}{\partial \boldsymbol{t}}+\boldsymbol{V}_{\boldsymbol{T}}\frac{\partial \boldsymbol{T}_0}{\partial \boldsymbol{x}}-\boldsymbol{D}_{\boldsymbol{T}}\frac{\partial^2 \boldsymbol{T}_0}{\partial \boldsymbol{x}^2}=\boldsymbol{k}_{\boldsymbol{off}}\boldsymbol{C}-\boldsymbol{k}_{\boldsymbol{on}}\boldsymbol{L}\boldsymbol{T}_0=-\frac{\partial \boldsymbol{C}}{\partial \boldsymbol{t}}-\boldsymbol{V}_{\boldsymbol{C}}\frac{\partial \boldsymbol{C}}{\partial \boldsymbol{x}}+\boldsymbol{D}_{\boldsymbol{C}}\frac{\partial^2 \boldsymbol{C}}{\partial \boldsymbol{x}^2}\,(1.1)$$

where $\boldsymbol{L}$, $\boldsymbol{T_0}$, $\boldsymbol{C}$ - concentrations of ligand, target and complex, respectively, $\boldsymbol{V_L}$, $\boldsymbol{V_T}$, $\boldsymbol{V_C}$ - electrophoretic velocities of these reactants, $\boldsymbol{D_L}$, $\boldsymbol{D_T}$, $\boldsymbol{D_C}$ - diffusion coefficients, $\boldsymbol{t}$ - time, $\boldsymbol{x}$ - a space coordinate, $\boldsymbol{k_{off}}$ - a decay rate constant, $\boldsymbol{k_{on}}$ - a rate constant of complex formation. Here, we start to discuss a special case of a sharp peak of the ligand and complex moving in a capillary with a initial concentration of target $\boldsymbol{T}$. With the small difference between total concentration of the target and initial concentration ($\vartheta \equiv \boldsymbol{T}_0 - \boldsymbol{T}$), we have the following equations:

$$\frac{\partial \boldsymbol{L}}{\partial \boldsymbol{t}}+\boldsymbol{V}_{\boldsymbol{L}}\frac{\partial \boldsymbol{L}}{\partial \boldsymbol{x}}-\boldsymbol{D}_{\boldsymbol{L}}\frac{\partial^2 \boldsymbol{L}}{\partial \boldsymbol{x}^2}=\frac{\partial \vartheta}{\partial \boldsymbol{t}}+\boldsymbol{V}_{\boldsymbol{T}}\frac{\partial \vartheta}{\partial \boldsymbol{x}}-\boldsymbol{D}_{\boldsymbol{T}}\frac{\partial^2 \vartheta}{\partial \boldsymbol{x}^2}=\boldsymbol{k}_{\boldsymbol{off}}\boldsymbol{C}-\boldsymbol{k}_{\boldsymbol{on}}\boldsymbol{L}\left(\boldsymbol{T}+\vartheta\right)=-\frac{\partial \boldsymbol{C}}{\partial \boldsymbol{t}}-\boldsymbol{V}_{\boldsymbol{C}}\frac{\partial \boldsymbol{C}}{\partial \boldsymbol{x}}+\boldsymbol{D}_{\boldsymbol{C}}\frac{\partial^2 \boldsymbol{C}}{\partial \boldsymbol{x}^2}\,(1.2)$$

These equations can be simplified in a few cases:

A. When the mobilities of the complex and the target are practically equal and diffusion coefficients play no significant role:

$$\boldsymbol{V}_{\boldsymbol{T}}=\boldsymbol{V}_{\boldsymbol{C}},\quad \boldsymbol{D}_{\boldsymbol{T}}=\boldsymbol{D}_{\boldsymbol{C}}=\boldsymbol{D}_{\boldsymbol{L}}=0\,(1.3)$$

For this case, using variable $\boldsymbol{P}\equiv\boldsymbol{C}+\vartheta$, we can obtain equations:

$$\begin{aligned}&\frac{\partial \boldsymbol{P}}{\partial \boldsymbol{t}}+\boldsymbol{V}_{\boldsymbol{T}}\frac{\partial \boldsymbol{P}}{\partial \boldsymbol{x}}=0\\&\frac{\partial \boldsymbol{L}}{\partial \boldsymbol{t}}+\boldsymbol{V}_{\boldsymbol{L}}\frac{\partial \boldsymbol{L}}{\partial \boldsymbol{x}}=\boldsymbol{k}_{\boldsymbol{off}}\left(\boldsymbol{P}-\vartheta\right)-\boldsymbol{k}_{\boldsymbol{on}}\boldsymbol{L}\left(\boldsymbol{T}+\vartheta\right)=\frac{\partial \vartheta}{\partial \boldsymbol{t}}+\boldsymbol{V}_{\boldsymbol{T}}\frac{\partial \vartheta}{\partial \boldsymbol{x}}\end{aligned}\qquad(1.4)$$

Further simplification can be made by using Cole-Hopf transformation. New variable $\boldsymbol{w}$ is connected with initial variables by the expression:

$$\boldsymbol{L}=\frac{\partial \boldsymbol{w}}{\partial \boldsymbol{t}}+\boldsymbol{V}_{\boldsymbol{T}}\frac{\partial \boldsymbol{w}}{\partial \boldsymbol{x}},\quad \vartheta=\frac{\partial \boldsymbol{w}}{\partial \boldsymbol{t}}+\boldsymbol{V}_{\boldsymbol{L}}\frac{\partial \boldsymbol{w}}{\partial \boldsymbol{x}}\,(1.5)$$

where $\boldsymbol{w}$ can be described as:

$$\left(\left(\frac{\partial}{\partial \boldsymbol{t}}+\boldsymbol{V}_{\boldsymbol{L}}\frac{\partial}{\partial \boldsymbol{x}}\right)\left(\frac{\partial}{\partial \boldsymbol{t}}+\boldsymbol{V}_{\boldsymbol{T}}\frac{\partial}{\partial \boldsymbol{x}}\right)+\boldsymbol{k}_{\boldsymbol{off}}\left(\frac{\partial}{\partial \boldsymbol{t}}+\boldsymbol{V}_{\boldsymbol{L}}\frac{\partial}{\partial \boldsymbol{x}}\right)+\boldsymbol{k}_{\boldsymbol{on}}\boldsymbol{T}\left(\frac{\partial}{\partial \boldsymbol{t}}+\boldsymbol{V}_{\boldsymbol{T}}\frac{\partial}{\partial \boldsymbol{x}}\right)-\boldsymbol{k}_{\boldsymbol{off}}\boldsymbol{P}\right)\exp\left(\boldsymbol{k}_{\boldsymbol{on}}\boldsymbol{w}\right)=0\,(1.6)$$

B. This is the case of big decay constant $\boldsymbol{k_{off}}$ and weak nonlinearity, when target concentration is changed slowly by the ligand and complex, $|\vartheta| \ll \boldsymbol{T}$. Diffusion coefficients are not zero but small. In this case, the equations can be rewritten as:

$$\begin{aligned}&\frac{\partial\left(\boldsymbol{L}+\boldsymbol{C}\right)}{\partial \boldsymbol{t}}+\frac{\partial\left(\boldsymbol{V}_{\boldsymbol{L}}\boldsymbol{L}+\boldsymbol{V}_{\boldsymbol{C}}\boldsymbol{C}\right)}{\partial \boldsymbol{x}}=\frac{\partial^2\left(\boldsymbol{D}_{\boldsymbol{L}}\boldsymbol{L}+\boldsymbol{D}_{\boldsymbol{C}}\boldsymbol{C}\right)}{\partial \boldsymbol{x}^2},\quad \boldsymbol{C}=\frac{1}{1+\frac{1}{\boldsymbol{k}_{\boldsymbol{off}}}\left(\frac{\partial}{\partial \boldsymbol{t}}+\boldsymbol{V}_{\boldsymbol{C}}\frac{\partial}{\partial \boldsymbol{x}}-\boldsymbol{D}_{\boldsymbol{C}}\frac{\partial^2}{\partial \boldsymbol{x}^2}\right)}\boldsymbol{L}\frac{\boldsymbol{T}+\vartheta}{\boldsymbol{K}_{\boldsymbol{d}}}\\&\vartheta=\left(1+\frac{\left(\boldsymbol{V}_{\boldsymbol{L}}-\boldsymbol{V}_{\boldsymbol{T}}\right)\frac{\partial}{\partial \boldsymbol{x}}-\left(\boldsymbol{D}_{\boldsymbol{L}}-\boldsymbol{D}_{\boldsymbol{T}}\right)\frac{\partial^2}{\partial \boldsymbol{x}^2}}{\frac{\partial}{\partial \boldsymbol{t}}+\boldsymbol{V}_{\boldsymbol{T}}\frac{\partial}{\partial \boldsymbol{x}}-\boldsymbol{D}_{\boldsymbol{T}}\frac{\partial^2}{\partial \boldsymbol{x}^2}}\right)\boldsymbol{L}\end{aligned}\qquad(1.7)$$

In the first order by small values, it can be simplified to:

$$C \approx T\frac{L}{K_d} - \frac{T}{k_{off}K_d}\left(\frac{\partial}{\partial t} + V_C\frac{\partial}{\partial x} - D_C\frac{\partial^2}{\partial x^2}\right)L + \frac{\vartheta L}{K_d}, \quad \vartheta \approx \left(1 + \frac{(V_L - V_T)\frac{\partial}{\partial x}}{\frac{\partial}{\partial t} + V_T\frac{\partial}{\partial x}}\right)L$$
$$\frac{\partial L\left(1+\frac{T}{K_d}\right)}{\partial t} + \frac{\partial\left(V_L + V_C\frac{T}{K_d}\right)L}{\partial x} + \left(\frac{\partial}{\partial t} + V_C\frac{\partial}{\partial x}\right)\frac{\vartheta L}{K_d} \approx \left(\frac{\partial^2\left(D_L + D_C\frac{T}{K_d}\right)}{\partial x^2} + \frac{T}{k_{off}K_d}\left(\frac{\partial}{\partial t} + V_C\frac{\partial}{\partial x}\right)^2\right)L \quad (1.8)$$

By introducing new variables:

$$V_{EM} \equiv \frac{V_L K_d + V_C T}{K_d + T}, D_{EM} \equiv \frac{D_L K_d + D_C T}{K_d + T} \quad (1.9)$$

and using the approximate expression that is correct in the zero order:

$$\frac{\partial}{\partial t} \approx -V_{EM}\frac{\partial}{\partial x} \quad (1.10)$$

We can finally obtain:

$$\left(\frac{\partial L}{\partial t} + V_{EM}\frac{\partial L}{\partial x}\right) + \frac{(V_C - V_{EM})(V_L - V_{EM})}{(V_T - V_{EM})(K_d + T)}\frac{\partial}{\partial x}L^2 \approx \left(D_{EM} + \frac{T(V_C - V_{EM})^2}{k_{off}(K_d + T)}\right)\frac{\partial^2}{\partial x^2}L \quad (1.11)$$

In addition:

$$C \approx T\frac{L}{K_d} - \frac{T(V_C - V_{EM})}{k_{off}K_d}\frac{\partial L}{\partial x} + \frac{L^2}{K_d}\frac{V_L - V_{EM}}{V_T - V_{EM}}, \quad \vartheta \approx \frac{V_L - V_{EM}}{V_T - V_{EM}}L \quad (1.12)$$

For the summarized concentration of ligand and complex $P \equiv L + C$, the equation is following:

$$L \approx \frac{K_d}{K_d + T}P + \frac{TK_d(V_C - V_{EM})}{k_{off}(K_d + T)^2}\frac{\partial}{\partial x}P + \frac{P^2K_d^2}{(K_d + T)^3}\frac{V_L - V_{EM}}{V_T - V_{EM}}$$
$$\left(\frac{\partial}{\partial t} + V_{EM}\frac{\partial}{\partial x}\right)P + \frac{K_d(V_C - V_{EM})(V_L - V_{EM})}{(V_T - V_{EM})(K_d + T)^2}\frac{\partial}{\partial x}P^2 \approx \left(D_{EM} + \frac{T(V_C - V_{EM})^2}{k_{off}(K_d + T)}\right)\frac{\partial^2}{\partial x^2}P \quad (1.13)$$

Equation (1.13) can be rewritten using expressions for their coefficients:

$$G \equiv \frac{K_d(V_C - V_{EM})(V_L - V_{EM})}{(V_T - V_{EM})(K_d + T)^2} = \frac{TK_d^2(V_C - V_L)^2}{(V_{EM} - V_T)(K_d + T)^4}$$
$$D_{CID} \equiv \frac{T(V_C - V_{EM})^2}{k_{off}(K_d + T)} = \frac{TK_d^2(V_C - V_L)^2}{k_{off}(K_d + T)^3} \quad (1.14)$$

Finally:

$$\left(\frac{\partial}{\partial t} + V_{EM}\frac{\partial}{\partial x}\right)P + G\frac{\partial}{\partial x}P^2 \approx (D_{EM} + D_{CID})\frac{\partial^2}{\partial x^2}P \quad (1.15)$$

This equation can be transformed into a linear diffusion equation using standard Cole-Hopf transformation:

$$\boldsymbol{P}(\boldsymbol{x},\boldsymbol{t}) \equiv -\frac{\partial}{\partial \boldsymbol{x}} \frac{\boldsymbol{D_{EM}} + \boldsymbol{D_{CID}}}{\boldsymbol{G}} \ln\left(\Theta_0 + \int_{-\infty}^{\boldsymbol{x}} \boldsymbol{Q}(\boldsymbol{x}',\boldsymbol{t}) d\boldsymbol{x}' \right),$$
$$\boldsymbol{Q}(\boldsymbol{x},\boldsymbol{t}) = \frac{\partial}{\partial \boldsymbol{x}} \exp\left(\frac{-\boldsymbol{G}}{\boldsymbol{D_{EM}} + \boldsymbol{D_{CID}}} \int_{-\infty}^{\boldsymbol{x}} \boldsymbol{P}(\boldsymbol{x}',\boldsymbol{t}) d\boldsymbol{x}' \right) \quad (1.16)$$

For Cole-Hopf variable $\boldsymbol{Q}$, a linear equation is satisfied:

$$\left(\frac{\partial}{\partial \boldsymbol{t}} + \boldsymbol{V_{EM}} \frac{\partial}{\partial \boldsymbol{x}} \right) \boldsymbol{Q} \approx \left(\boldsymbol{D_{EM}} + \boldsymbol{D_{CID}} \right) \frac{\partial^2}{\partial \boldsymbol{x}^2} \boldsymbol{Q} \quad (1.17)$$

2. Partial solutions

The simplest solution of the equation (1.17) has a form:

$$\boldsymbol{Q} \square \boldsymbol{Q}_0 + \frac{1}{\sqrt{\pi\left(\Delta_0^2 + 4\boldsymbol{t}\left(\boldsymbol{D_{EM}} + \boldsymbol{D_{CID}} \right) \right)}} \exp\left(-\frac{\left(\boldsymbol{x} - \boldsymbol{V_{EM}}\boldsymbol{t} \right)^2}{\Delta_0^2 + 4\boldsymbol{t}\left(\boldsymbol{D_{EM}} + \boldsymbol{D_{CID}} \right)} \right) \quad (2.1)$$

The total concentration of bound and free ligand after Cole-Hopf transformation is corresponded to:

$$\boldsymbol{P}(\boldsymbol{x},\boldsymbol{t}) \equiv \frac{\boldsymbol{D_{EM}} + \boldsymbol{D_{CID}}}{|\boldsymbol{G}|\Delta} \frac{\exp\left(-\frac{\left(\boldsymbol{x} - \boldsymbol{V_{EM}}\boldsymbol{t} \right)^2}{\Delta} \right)}{\left| \sqrt{\pi}\boldsymbol{B} + \int_{-\infty \cdot \boldsymbol{sign}(\boldsymbol{V_T} - \boldsymbol{V_{EM}})}^{\frac{(\boldsymbol{x} - \boldsymbol{V_{EM}}\boldsymbol{t})}{\Delta}} \exp\left(-\boldsymbol{x}^2 \right) d\boldsymbol{x} \right|} =$$
$$= \frac{\left(1 + \frac{\boldsymbol{D_{EM}}}{\boldsymbol{D_{CID}}} \right)\left(\boldsymbol{K_d} + \boldsymbol{T} \right)|\boldsymbol{V_T} - \boldsymbol{V_{EM}}|}{\boldsymbol{k_{off}}\Delta} \frac{\exp\left(-\left(\frac{\boldsymbol{x} - \boldsymbol{V_{EM}}\boldsymbol{t}}{\Delta} \right)^2 \right)}{\left| \sqrt{\pi}\boldsymbol{B} + \int_{-\infty \cdot \boldsymbol{sign}(\boldsymbol{V_T} - \boldsymbol{V_{EM}})}^{\frac{(\boldsymbol{x} - \boldsymbol{V_{EM}}\boldsymbol{t})}{\Delta}} \exp\left(-\boldsymbol{x}^2 \right) d\boldsymbol{x} \right|} \quad (2.2)$$

where Δ is defined as:

$$\Delta \equiv \sqrt{\Delta_0^2 + 4\boldsymbol{t}\left(\boldsymbol{D_{EM}} + \boldsymbol{D_{CID}} \right)} \quad (2.3)$$

The total amount of bounded and free ligand $L_0 \times \boldsymbol{l}$ per unit of a capillary section area is:

$$L_0 \times \boldsymbol{l} \equiv \int_{-\infty}^{\infty} \boldsymbol{P}(\boldsymbol{x}) d\boldsymbol{x} = \frac{1}{\boldsymbol{k_{off}}} \left(1 + \frac{\boldsymbol{D}}{\boldsymbol{D_{CID}}} \right)\left(\boldsymbol{K_d} + \boldsymbol{T} \right)|\boldsymbol{V_T} - \boldsymbol{V}| \ln\left(1 + \frac{1}{\boldsymbol{B}} \right) \quad (2.4)$$

According (2.4),

$$\boldsymbol{B} = 1 / \left(\exp\left(\frac{\boldsymbol{k_{off}}\boldsymbol{D_{CID}} L_0 \times \boldsymbol{l}}{|\boldsymbol{V_T} - \boldsymbol{V}|\left(\boldsymbol{K_d} + \boldsymbol{T} \right)\left(\boldsymbol{D_{CID}} + \boldsymbol{D} \right)} \right) - 1 \right) \quad (2.5)$$

3. Initial conditions

Initial condition corresponds to a rectangular plug with length, $\boldsymbol{l}$, and the sum concentration of the ligand and complex, L_0. After Cole – Hopf transformation (1.16) the initial condition for equation (1.17) has a form:

$$\boldsymbol{Q}(\boldsymbol{x},0)=-\frac{\boldsymbol{G}\mathrm{L}_0\theta(\boldsymbol{x})\theta(\boldsymbol{l}-\boldsymbol{x})}{\boldsymbol{D}_{\boldsymbol{EM}}+\boldsymbol{D}_{\boldsymbol{CID}}}\exp\left(\frac{-\boldsymbol{G}\mathrm{L}_0\boldsymbol{x}}{\boldsymbol{D}_{\boldsymbol{EM}}+\boldsymbol{D}_{\boldsymbol{CID}}}\right)\quad(3.1)$$

Mean square of coordinates for distribution (3.1) is

$$2\left\langle\delta\boldsymbol{x}^2\right\rangle=2\left(\frac{\boldsymbol{l}}{\lambda}\right)^2\left(\frac{\int_0^\lambda\exp(\boldsymbol{x})\,\boldsymbol{x}^2\boldsymbol{dx}}{\int_0^\lambda\exp(\boldsymbol{x})\,\boldsymbol{dx}}-\left(\frac{\int_0^\lambda\exp(\boldsymbol{x})\,\boldsymbol{x}\boldsymbol{dx}}{\int_0^\lambda\exp(\boldsymbol{x})\,\boldsymbol{dx}}\right)^2\right)\quad(3.2)$$

where λ is defined as:

$$|\lambda|\equiv\left|\frac{\boldsymbol{G}\mathrm{L}_0\times\boldsymbol{l}}{\boldsymbol{D}_{\boldsymbol{EM}}+\boldsymbol{D}_{\boldsymbol{CID}}}\right|=\left|\frac{\boldsymbol{k}_{\boldsymbol{off}}\mathrm{L}_0\times\boldsymbol{l}}{(1+\boldsymbol{D}_{\boldsymbol{EM}}/\boldsymbol{D}_{\boldsymbol{CID}})(\boldsymbol{K}_{\boldsymbol{d}}+\boldsymbol{T})(\boldsymbol{V}_{\boldsymbol{T}}-\boldsymbol{V}_{\boldsymbol{EM}})}\right|\quad(3.3)$$

equation (3.2) can be transformed as

$$2\left\langle\delta\boldsymbol{x}^2\right\rangle=2\left(\frac{\boldsymbol{l}}{\lambda}\right)^2\left(1-\left(\frac{\lambda/2}{\sinh(\lambda/2)}\right)^2\right)\quad(3.4)$$

According to (1.17), value (3.4) is equal to value Δ_0^2 in expressions (2.1) and (2.3). Mean square of coordinates in diffusion process always depends on time exactly the same as for Gaussian peaks, and an every peak becomes near Gaussian with time. Finally, for Δ_0 we can have:

$$\Delta_0=\sqrt{2}\left|\frac{\boldsymbol{l}}{\lambda}\right|\sqrt{1-\left(\frac{\lambda/2}{\sinh(\lambda/2)}\right)^2}\quad(3.5)$$

4. Peaks fitting

According to (2.2), the form of a peak in an electropherogram can be described as:

$$\rho(\boldsymbol{t})=\frac{\boldsymbol{A}\exp\left(-(\boldsymbol{t}-\boldsymbol{t}_0)^2/\boldsymbol{w}^2\right)}{\boldsymbol{w}\left|\sqrt{\pi}\boldsymbol{B}+\int_{-\infty\cdot\boldsymbol{sign}(\boldsymbol{V}_{\boldsymbol{T}}-\boldsymbol{V}_{\boldsymbol{EM}})}^{(\boldsymbol{t}-\boldsymbol{t}_0)/\boldsymbol{w}}\exp\left(-\boldsymbol{x}^2\right)\boldsymbol{dx}\right|}\quad(4.1)$$

We need to know parameters $\boldsymbol{t}_0$, $\boldsymbol{A}$, $\boldsymbol{w}$ and $\boldsymbol{J}\equiv\ln\left(1+\frac{1}{|\boldsymbol{B}|}\right)$ for proper describing the form of the peak. The direct way to determine these parameters is the fitting the form of the peak.

We can also find these parameters without peak fitting by following steps:

1. $\boldsymbol{A}$ can be found from the expression:

$$\boldsymbol{A}=\int_{-\infty}^{\infty}\rho(\boldsymbol{t})\boldsymbol{dt}\quad(4.2)$$

2. For a sharp peak, $\boldsymbol{t}_0$ corresponds to peak's maximum. It becomes precise for big enough $\boldsymbol{B}$, but possible imprecision play no practical role. This parameter is in use for $\boldsymbol{K}_{\boldsymbol{d}}$ determination, and possible relative error as a result of imprecision is not higher the ratio of peak width on the electropherogram to $\boldsymbol{t}_0$.
3. For big $\boldsymbol{B}$ what means small $\boldsymbol{J}$, parameter $\boldsymbol{w}$ can be found from expression

$$\boldsymbol{w}=\sqrt{2\left\langle\delta\boldsymbol{t}^2\right\rangle}\quad(4.3)$$

For arbitrary $\boldsymbol{B}$, (4.3) can be generalized to expression

$$\boldsymbol{w} = \sqrt{2\left\langle \delta \boldsymbol{t}^2 \right\rangle} / \Phi\left(\boldsymbol{J}(\boldsymbol{B})\right) \quad (4.4)$$

where function $\Phi(\boldsymbol{J})$ is defined by the expressions:

$$\Phi(\boldsymbol{B}) \equiv \sqrt{\frac{\int_{-\infty}^{\infty} \tau^2 \rho(\tau)\, \boldsymbol{d}\tau}{\int_{-\infty}^{\infty} \rho(\tau)\, \boldsymbol{d}\tau} - \left(\frac{\int_{-\infty}^{\infty} \tau \rho(\tau)\, \boldsymbol{d}\tau}{\int_{-\infty}^{\infty} \rho(\tau)\, \boldsymbol{d}\tau} \right)^2} \quad (4.5)$$

where

$$\rho(\tau) \equiv \frac{\partial}{\partial \tau} \ln\left(\sqrt{\pi}\,|\boldsymbol{B}| + \int_{-\infty}^{\tau} \exp\left(-\boldsymbol{x}^2\right) \boldsymbol{dx} \right) \quad (4.6)$$

The approximate expression for the function $\Phi(\boldsymbol{J})$ can be found numerically and has a form:

$$\Phi(\boldsymbol{J}) \approx (1 + \boldsymbol{J}^{1.88159722011194} / 31.8307184800561)^{0.23611765995013} \quad (4.7)$$

4. For finding peak's asymmetry, $\boldsymbol{J}$, a ratio of peak's subareas before and after its maximum can be used. For expression (4.6) describing the shape of the peak, the position of peak's maximum, $\boldsymbol{z}$, is satisfied to the following equation:

$$\partial_{\boldsymbol{z}} \rho(\boldsymbol{z}) = -\left(2\boldsymbol{z} + \rho(\boldsymbol{z})\right) \rho(\boldsymbol{z}) = 0 \Rightarrow 2\boldsymbol{z} + \rho(\boldsymbol{z}) = 0 \quad (4.8)$$

According to (4.6) and (4.8)

$$\frac{\exp(-\boldsymbol{z}^2)}{2\boldsymbol{z}} + \int_{-\infty}^{\boldsymbol{z}} \exp(-\boldsymbol{y}^2) \boldsymbol{dy} = -\boldsymbol{B}\sqrt{\pi} \quad (4.9)$$

Subareas are integrals of (4.6) before and after $\boldsymbol{z}$. The ratio of a bigger subarea to smaller subarea, $\boldsymbol{r}$, can be expressed as a function of $\boldsymbol{J}$:

$$\boldsymbol{r} = \frac{\boldsymbol{J}}{\ln\left(1 + \frac{\exp(\boldsymbol{J}) - 1}{\sqrt{\pi}} \int_{-\infty}^{\boldsymbol{z}} \exp(-\boldsymbol{y}^2) \boldsymbol{dy}\right)} - 1 \quad (4.10)$$

Based on (4.10), the approximated connection between $\boldsymbol{J}$ and $\boldsymbol{r}$ can be found as:

$$\boldsymbol{J} \approx 5.49902754 \cdot (\boldsymbol{r} - 1)^{0.879250897} \cdot \exp\left((\boldsymbol{r} - 1) \cdot 0.028860911\right) \quad (4.11)$$

5. Constants determinations

According to (4.1), if two peaks are different only by their widths and asymmetries, then the square difference between them will be

$$\boldsymbol{H}\left(\boldsymbol{w}_1, \boldsymbol{B}_1, \boldsymbol{w}_2, \boldsymbol{B}_2\right) = \int \left(\frac{\rho\left(\boldsymbol{t}, \boldsymbol{t}_0, \boldsymbol{A}, \boldsymbol{w}_1, \boldsymbol{B}_1\right)}{\int_{-\infty}^{\infty} \rho\left(\boldsymbol{t}', \boldsymbol{t}_0, \boldsymbol{A}, \boldsymbol{w}_1, \boldsymbol{B}_1\right) \boldsymbol{dt}'} - \frac{\rho\left(\boldsymbol{t}, \boldsymbol{t}_0, \boldsymbol{A}, \boldsymbol{w}_2, \boldsymbol{B}_2\right)}{\int_{-\infty}^{\infty} \rho\left(\boldsymbol{t}', \boldsymbol{t}_0, \boldsymbol{A}, \boldsymbol{w}_2, \boldsymbol{B}_2\right) \boldsymbol{dt}'} \right)^2 \boldsymbol{dt} =$$

$$= \int \left(\frac{\partial}{\partial \boldsymbol{t}} \left(\frac{\ln\left(\sqrt{\pi}\boldsymbol{B}_1 + \int_{-\infty\cdot}^{\boldsymbol{t}/\boldsymbol{w}_1} \exp\left(-\boldsymbol{x}^2\right) \boldsymbol{dx} \right)}{\ln(1 + 1/\boldsymbol{B}_1)} - \frac{\ln\left(\sqrt{\pi}\boldsymbol{B}_2 + \int_{-\infty\cdot}^{\boldsymbol{t}/\boldsymbol{w}_2} \exp\left(-\boldsymbol{x}^2\right) \boldsymbol{dx} \right)}{\ln(1 + 1/\boldsymbol{B}_2)} \right) \right)^2 \boldsymbol{dt} \quad (5.1)$$

Expression (5.1) can be simplified when we define new variables:

$$\boldsymbol{w}=(\boldsymbol{w}_1+\boldsymbol{w}_2)/2,\quad \boldsymbol{B}=(\boldsymbol{B}_1+\boldsymbol{B}_2)/2,\quad \delta\boldsymbol{w}=(\boldsymbol{w}_1-\boldsymbol{w}_2)/2,\quad \delta\boldsymbol{B}=(\boldsymbol{B}_1-\boldsymbol{B}_2)/2 \quad (5.2)$$

And assume that difference between parameters $\delta\boldsymbol{w}$ and $\delta\boldsymbol{B}$ is small:

$$\boldsymbol{N}\equiv\sqrt{\pi}\boldsymbol{B}+\int_{-\infty}^{\boldsymbol{z}}\exp\left(-\boldsymbol{x}^2\right)\boldsymbol{dx},\quad \boldsymbol{F}\equiv\frac{\exp\left(-\boldsymbol{z}^2\right)}{\boldsymbol{N}},\quad \boldsymbol{J}\equiv\ln\left(1+\frac{1}{\boldsymbol{B}}\right)$$

$$\boldsymbol{H}\approx\frac{4}{\boldsymbol{w}}\int\left(\left(\frac{\partial}{\partial\boldsymbol{z}}\frac{\left(\sqrt{\pi}\delta\boldsymbol{B}-\frac{\boldsymbol{z}\delta\boldsymbol{w}}{\boldsymbol{w}}\exp\left(-\boldsymbol{z}^2\right)\right)}{\boldsymbol{NJ}}+\frac{\delta\boldsymbol{BF}}{\boldsymbol{B}^2\boldsymbol{J}^2}\right)\right)^2\boldsymbol{dz}= \quad (5.3)$$

$$=\frac{4}{\boldsymbol{wJ}^2}\int\left(\boldsymbol{F}\left(\frac{\delta\boldsymbol{w}}{\boldsymbol{w}}\left(1-2\boldsymbol{z}^2-\boldsymbol{zF}\right)+\delta\boldsymbol{B}\left(\frac{\sqrt{\pi}}{\boldsymbol{N}}-\frac{1}{\boldsymbol{B}^2\boldsymbol{J}}\right)\right)\right)^2\boldsymbol{dz}\equiv$$

$$\equiv\boldsymbol{I}_0(\boldsymbol{J})\frac{\delta\boldsymbol{J}^2}{\boldsymbol{w}}+\boldsymbol{I}_1(\boldsymbol{J})\frac{\delta\boldsymbol{w}}{\boldsymbol{w}^2}\delta\boldsymbol{J}+\boldsymbol{I}_2(\boldsymbol{J})\frac{\delta\boldsymbol{w}^2}{\boldsymbol{w}^3}$$

where parameter $\boldsymbol{B}$ is connected with the asymmetry parameter $\boldsymbol{J}$:

$$\boldsymbol{B}=\frac{1}{\exp(\boldsymbol{J})-1},\quad \delta\boldsymbol{B}=-\frac{\delta\boldsymbol{J}}{4\sinh(\boldsymbol{J}/2)^2} \quad (5.4)$$

And used for definitions:

$$\boldsymbol{I}_0(\boldsymbol{J})\equiv\frac{1}{4\boldsymbol{J}^2\sinh(\boldsymbol{J}/2)^4}\int\left(\boldsymbol{F}\left(\frac{\sqrt{\pi}}{\boldsymbol{N}}-\frac{1}{\boldsymbol{B}^2\boldsymbol{J}}\right)\right)^2\boldsymbol{dz} \quad (5.5)$$

$$\boldsymbol{I}_2(\boldsymbol{J})\equiv\frac{4}{\boldsymbol{J}^2}\int\left(\boldsymbol{F}\left(1-2\boldsymbol{z}^2-\boldsymbol{zF}\right)\right)^2\boldsymbol{dz}$$

$$\boldsymbol{I}_1(\boldsymbol{J})\equiv\frac{-2}{\boldsymbol{J}^2\sinh(\boldsymbol{J}/2)^2}\int\boldsymbol{F}\left(\frac{\sqrt{\pi}}{\boldsymbol{N}}-\frac{1}{\boldsymbol{B}^2\boldsymbol{J}}\right)\boldsymbol{F}\left(1-2\boldsymbol{z}^2-\boldsymbol{zF}\right)\boldsymbol{dt}$$

Integrals (5.5) can be found numerically, as functions of $\boldsymbol{J}$, so approximate expressions for them are

$$\boldsymbol{I}_0(\boldsymbol{J})\approx\exp(-1.2528245054+0.4458595661\cdot\boldsymbol{J}+0.0783120873\cdot\boldsymbol{J}^2-0.0014341015\cdot\boldsymbol{J}^3)$$

$$\boldsymbol{I}_1(\boldsymbol{J})\approx\exp(-1.5332457793-0.0255243875\cdot\boldsymbol{J}+0.0472953261\cdot\boldsymbol{J}^2-0.0008175906\cdot\boldsymbol{J}^3) \quad (5.6)$$

$$\boldsymbol{I}_1(\boldsymbol{J})\approx\exp(-1.8876358911-0.6609871055\cdot\boldsymbol{J}+0.0300281253\cdot\boldsymbol{J}^2-0.0005155394\cdot\boldsymbol{J}^3)$$

For fitting of the parameters, total error for few experiments will be sum of the approximated expressions(5.3).

6. Confidence of the data in different experimental conditions

Variations of width and asymmetry are connected with variation $\boldsymbol{k_{off}}$ according the following expressions:

$$\delta\boldsymbol{J}=\boldsymbol{J}\frac{\delta\boldsymbol{k_{off}}}{\boldsymbol{k_{off}}},\quad \delta\boldsymbol{w}=-\frac{2\boldsymbol{tD_{CID}}}{\boldsymbol{w}}\frac{\delta\boldsymbol{k_{off}}}{\boldsymbol{k_{off}}} \quad (6.1)$$

Based on (6.1), (5.3) can be rewriting in the form of:

$$\boldsymbol{H} = \boldsymbol{S} \cdot \left(\frac{\delta \boldsymbol{k}_{off}}{\boldsymbol{k}_{off}} \right)^2, \quad \boldsymbol{S} = \boldsymbol{I}_0(\boldsymbol{J}) \frac{\boldsymbol{J}^2}{\boldsymbol{w}} - \boldsymbol{I}_1(\boldsymbol{J}) \frac{2\boldsymbol{t}\boldsymbol{J}\boldsymbol{D}_{EM}}{\boldsymbol{w}^3} + \boldsymbol{I}_2(\boldsymbol{J}) \frac{4\left(\boldsymbol{t}\boldsymbol{D}_{EM}\right)^2}{\boldsymbol{w}^5} \quad (6.2)$$

where $\boldsymbol{S}$ is confidence of the data. In **Figure S1**, the typical behavior of the confidence for β-CD/Ibuprofen complex formation is presented.

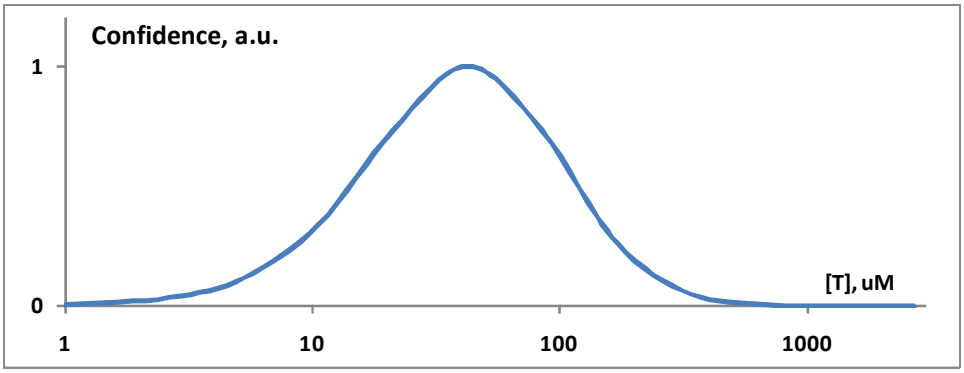

Figure S1. The behavior of the confidence for β-CD/Ibuprofen complex formation.

Table S1. β-CD/Ibuprofen complex formation parameters.

K_d, µM	83
k_{off}, s^{-1}	8,4
$[Ibuprofen]_0$, µM	30

$[\beta\text{-CD}]_0$, µM	**0**	**10**	**100**	**1000**	**2500**	**5000**
[Complex], µM	0	2.5	15.2	27.6	29.0	29.5
Relaxation time, ms	-	83.6	53.9	9.3	3.8	1.9
Complex's life time, ms	-	118.8	118.8	118.8	118.8	118.8
Unbound ibuprofen life time, ms	-	1,313.0	116.2	10.1	3.9	1.9
Unbound β-CD life time, ms	-	358.4	664.7	4,179.6	10,114.8	20,014.1

Table S2. β-CD/S-flurbiprofen complex formation parameters.

K_d, µM	155
k_{off}, s^{-1}:	32.6
$[S\text{-}Flurbiprofen]_0$, µM	30

$[\beta\text{-}CD]_0$, µM	**0**	**10**	**100**	**1000**	**2500**	**5000**
[Complex], µM	0	1.5	10.9	25.8	28.2	29.1
Relaxation time, ms	-	24.7	18.1	4.2	1.8	0.9
Complex's life time, ms	-	30.7	30.7	30.7	30.7	30.7
Unbound s-flurbiprofen life time, ms	-	562.7	53.3	4.8	1.9	0.9
Unbound β-CD life time, ms	-	167.1	249.5	1,154.5	2,685.8	5,241.2

Table S3. β-CD/Salicylic acid complex formation parameters.

Kd, µM	3215
k_{off}, s^{-1}:	4.3
$[Salicylic\ acid]_0$, µM	30

$[\beta\text{-}CD]_0$, µM	**0**	**10**	**100**	**1000**	**2500**	**5000**
[Complex], µM	0	0.1	0.8	7.1	13.1	18.2
Relaxation time, ms	-	229.7	223.6	176.7	130.7	91.1
Complex's life time, ms	-	232.6	232.6	232.6	232.6	232.6
Unbound salicylic acid life time, ms	-	75,462.9	7,544.4	753.0	300.6	150.1
Unbound β-CD life time, ms	-	24,999.3	25,690.7	32,619.5	44,200.9	63,540.8

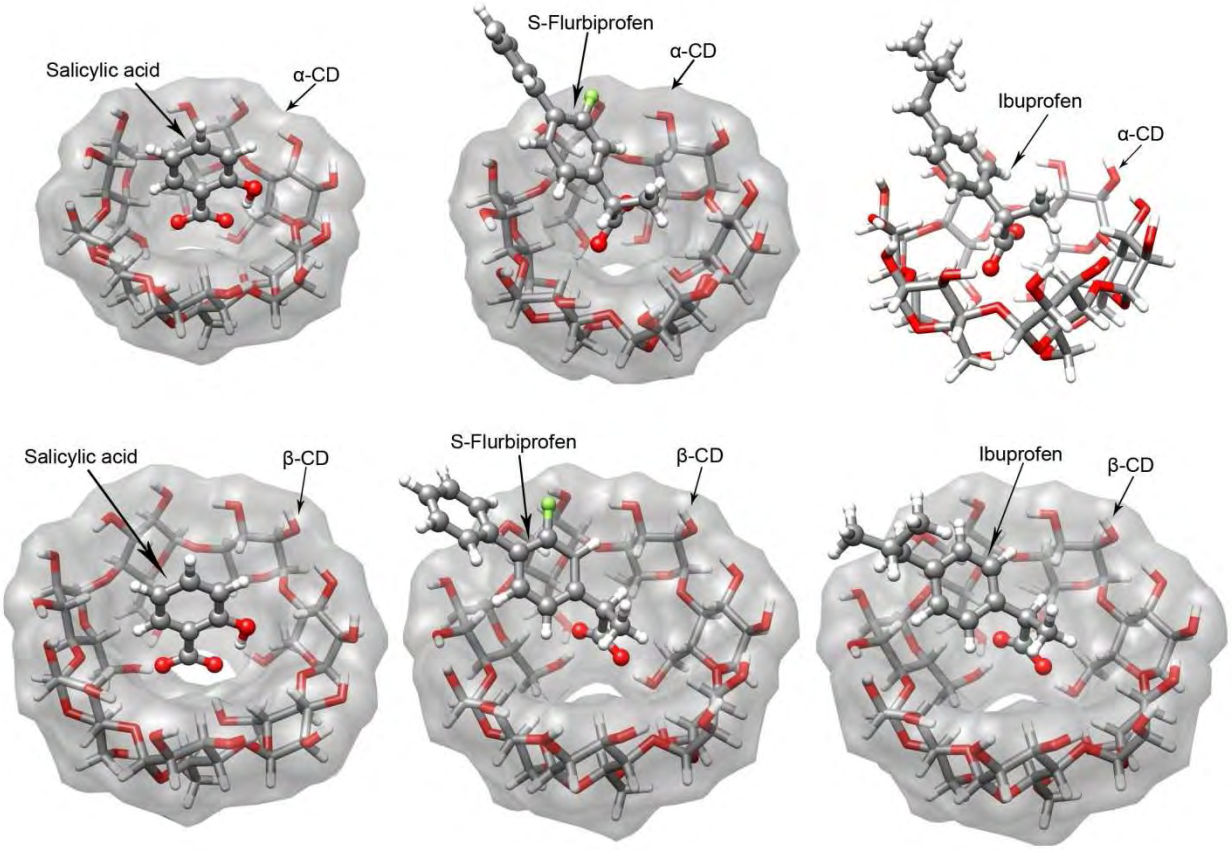

Figure S2. DFT-calculated structures of complexes of α- and β-cyclodextrins and small molecule drugs.

DFT COMPUTATIONAL DETAILS:

Density Functional Theory (DFT) calculations have been performed using the ***Gaussian 03*** program.[1] In all calculations, the spin-restricted method was employed. Wave function stability calculations were performed to confirm that the calculated wave functions corresponded to the electronic ground state. The structures of all species were optimized using the B3LYP exchange-correlation (XC) functional[2,3] with the DZVP[4] basis set. Tight SCF convergence criteria (10^{-8} a.u.) were used for all calculations. Where possible, harmonic frequency calculations with the analytic evaluation of force gradients (OPT=CalcAll) were used to determine the nature of the stationary points. The binding energies were evaluated at the same level of theory as the geometry optimization. Optimized structures of the complexes were visualized using UCSF Chimera.[5,6]

References

(1) Frisch, M. J.; Trucks, G. W.; Schlegel, H. B.; Scuseria, G. E.; Robb, M. A.; Cheeseman, J. R.; Montgomery, J., J. A. ; Vreven, T.; Kudin, K. N.; Burant, J. C.; Millam, J. M.; Lyengar, S. S.; Tomasi, J.; Barone, V.; Mennucci, B.; Cossi, M.; Scalmani, G.; Rega, N.; Petersson, G. A.; Nakatsuji, H.; Hada, M.; Ehara, M.; Toyota, K.; Fukuda, R.; Hasegawa, J.; Ishida, M.; Nakajima, T.; Honda, Y.; Kitao, O.; Nakai, H.; Klene, M.; Li, X.; Knox, J. E.; Hratchian, H. P.; Cross, J. B.; Adamo, C.; Jaramillo, J.; Gomperts, R.; Stratmann, R. E.; Yazyev, O.; Austin, A. J.; Cammi, R.; Pomelli, C.; Ochterski, J. W.; Ayala, P. Y.;

Morokuma, K.; Voth, G. A.; Salvador, P.; Dannenberg, J. J.; Zakrzewski, V. G.; Dapprich, S.; Daniels, A. D.; Strain, M. C.; Farkas, O.; Malick, D. K.; Rabuck, A. D.; Raghavachari, K.; Foresman, J. B.; Ortiz, J. V.; Cui, Q.; Baboul, A. G.; Clifford, S.; Cioslowski, J.; Stefanov, B. B.; Liu, G.; Liashenko, A.; Piskorz, P.; Komaromi, I.; Martin, R. L.; Fox, D. J.; Keith, T.; Al-Laham, M. A.; Peng, C. Y.; Nanayakkara, A.; Challacombe, M.; Gill, P. M. W.; Johnson, B.; Chen, W.; Wong, M. W.; Gonzalez, C.; Pople, J. A.; Gaussian, Inc.: 2003.
(2) Becke, A. D. ***Journal of Chemical Physics*** **1993**, ***98***, 5648.
(3) Lee, C.; Yang, W.; Parr, R. G. ***Physical Reviews*** **1988**, ***B37***, 785.
(4) Godbout, N.; Salahub, D. R.; Andzelm, J.; Wimmer, E. ***Canadian Journal of Chemistry*** **1992**, ***70***, 560-571.
(5) Pettersen, E. F.; Goddard, T. D.; Huang, C. C.; Couch, G. S.; Greenblatt, D. M.; Meng, E. C.; Ferrin, T. E. ***Journal of Computational Chemistry*** **2004**, ***25***, 1605-1612.
(6) Pettersen, E. F.; Goddard, T. D.; Huang, C. C.; Couch, G. S.; Greenblatt, D. M.; Meng, E. C.; Ferrin, T. E. San Francisco, 2005.